Fluid Dynamics Panel Method

ARO 3011-03

Basil Aranda
Computational Fluids Project

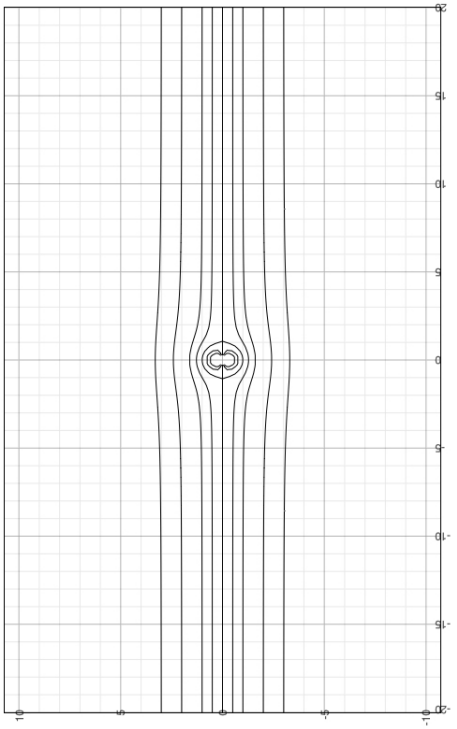

Aerospace Engineering
California State Polytechnic University, Pomona
24 November, 2021

Fluid Dynamics Panel Method ARO 3011

Basil Aranda[1]†

[1]Department of Aerospace Engineering, California State Polytechnic University, Pomona, 3801 W Temple Ave, Pomona, CA 91768

(Received xx; revised xx; accepted xx)

CONTENTS

1. Theory 2
2. Pressure Coefficient Plots and Figures 6
3. Table 10
4. Summary Sketch 16
5. Streamline Pattern Plots 17
5.1. Pressure Coefficient Theory V. Actual 21
6. Citations 22
Appendix A 24
Appendix B 25

Executive Summary

Computational Fluid Dynamics is an important part of aerospace theory and a growing field of research as faster, quicker, and more efficient wing panels are invented. For this lowspeed fluid dynamics class we were tasked with modelling a cylinder utilizing the source panel method.

The underlying theory is that an object, in this case a cylinder, may be approximated as a series of panels, N, with the same length as it 'contours' the intended object. The iterative process is very foundational and is used in conjunction with various aerodynamic theories including *Bernoulli's Method*. Included are different circulation values for $K = 0, -1, -2$, and -3. By first determining control points and angular components, it was possible to ascertain the coefficient of pressure, *Cp*. Using this data, it was also possible to plot streamlines for the function to visualize field flow around the cylinder. The principle of superposition is clearly outlined while the streamline plots also clearly show that there is flow separation at the back of the cylinder where the streamlines do not follow the surface curvature. It follows then, that maximum speed would occur at both the top and bottom of the cylinder with stagnation points at $\theta = 0$ and $\theta = \pi$ when $\Gamma = 0$. Of course, this could be an application of *d'Alembert's Paradox* where the drag is zero of a closed, two-dimensional body with incompressible and inviscid flow.

The computer simulation and plotting provided very nice results which were then tabulated and graphed. The theoretical and actual pressure coefficients were then compared and a percent error found between both. As expected, the percent error is extremely low and as the number of panels increase, so too does the accuracy. It was also possible to better visually recognize the effect that circulation has on *Cp*.

Altogether this was a very educational project and a fantastic application to theory learned in lecture.

† Email address for correspondence: boaranda@cpp.edu

1. Theory

Equations and Definition Figure

$$\zeta_i = \frac{1}{2} * (x_i + x_{i+1}) \tag{1.1}$$

Zeta is the control point midway between consecutive x terms.

$$\eta_i = \frac{1}{2} * (y_i + y_{i+1}) \tag{1.2}$$

Eta is the control point midway between consecutive y terms.

$$\theta_i = \arctan \frac{y_{i+1} - y_i}{x_{i+1} - x_i} \tag{1.3}$$

Theta is the angle defined between consecutive x and y terms

$$r_{ij} = \sqrt{(\zeta_j - \zeta_i)^2 + (\eta_j - \eta_i)^2} \tag{1.4}$$

r is a 2-dimensional array that refers to the magnitude length of consecutive ζ and η terms

$$\phi_i = \arctan \frac{\eta_j - \eta_i}{\zeta_j - \zeta_i} \tag{1.5}$$

Phi utilizes ζ and η as defined in lecture

$$\Delta s_j = \sqrt{(y_{j+1} + y_j)^2 + (x_{j+1} + x_j)^2} \tag{1.6}$$

Δs_j is simply the magnitude of consective x and y control points. It also forms the panel length. Therefore, the panel length must also be equal around the cylinder.

$$\Delta s = 2R \sin(\frac{\beta}{2}) \tag{1.7}$$

Δs_j Alternate equation to the above

$$Cp(i) = 1 - \frac{[V_{tan}(i)]^2}{V_{inf}^2} \tag{1.8}$$

Coefficient of Pressure is found to be 1 minus the difference between Vtan and Vinf

$$B(i) = \overline{n}(i) \cdot \overline{V}_{inf} \tag{1.9}$$

$$A(i,j) = \frac{q(j)s(j)\overline{R}(i,j)}{2\pi[R(i,j)]^2} \tag{1.10}$$

$$A(i,j) = \frac{1}{2s(i)} \tag{1.11}$$

Key Equations

$$C_{ij} = \frac{\sin(\theta_i - \phi_{ij})}{2\pi r_{ij}} * \Delta s_j \tag{1.12}$$

This equation is used to create the 2-dimensional matrix used to find λ

$$\overline{C_{ij}} = \frac{\cos(\theta_i - \phi_{ij})}{2\pi r_{ij}} * \Delta s_j \tag{1.13}$$

This equation is used in conjunction with λ to find Vtan

$$p_s = p_o + \frac{1}{2}\rho U^2 * (1 - 4\sin(\theta)^2 + \frac{2\Gamma \sin(\theta)}{\pi a U} - \frac{\Gamma^2}{4\pi^2 a^2 U^2}) \tag{1.14}$$

$$\Psi = Ur(1 - \frac{a^2}{r^2}) * \sin(\theta) - \frac{\Gamma}{2\pi}\ln r \tag{1.15}$$

Stream function

$$\phi = Ur(1 + \frac{a^2}{r^2}) * \cos(\theta) + \frac{\Gamma}{2\pi}\ln r \tag{1.16}$$

Velocity Potential

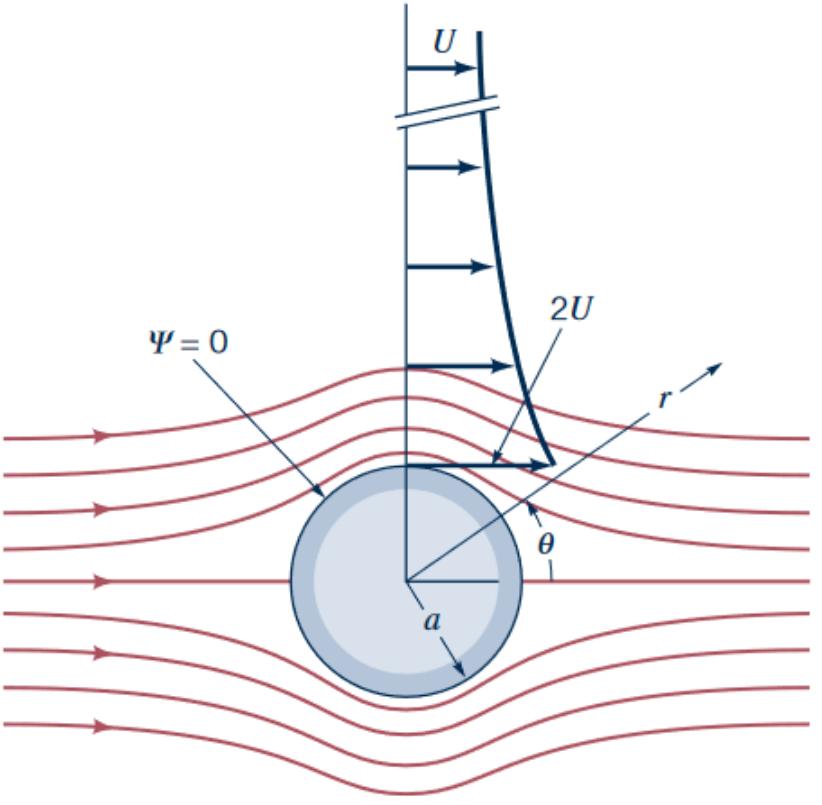

FIGURE 1. Definition Picture

Munson 8^{th} Edition

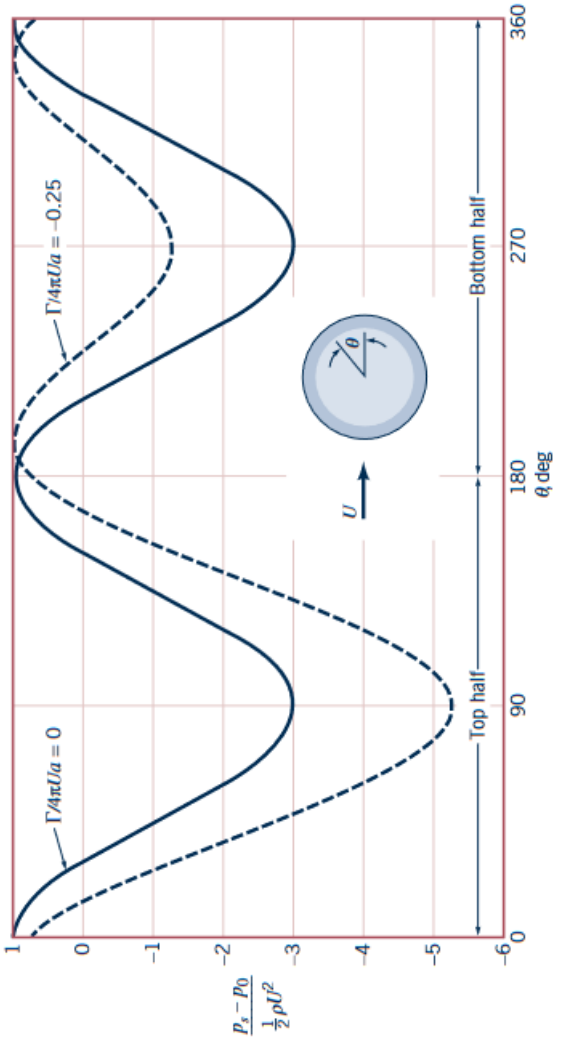

FIGURE 2. Cylinder With and Without Rotation

Munson 8^{th} Edition

2. Pressure Coefficient Plots and Figures

N = 250 and K = 0

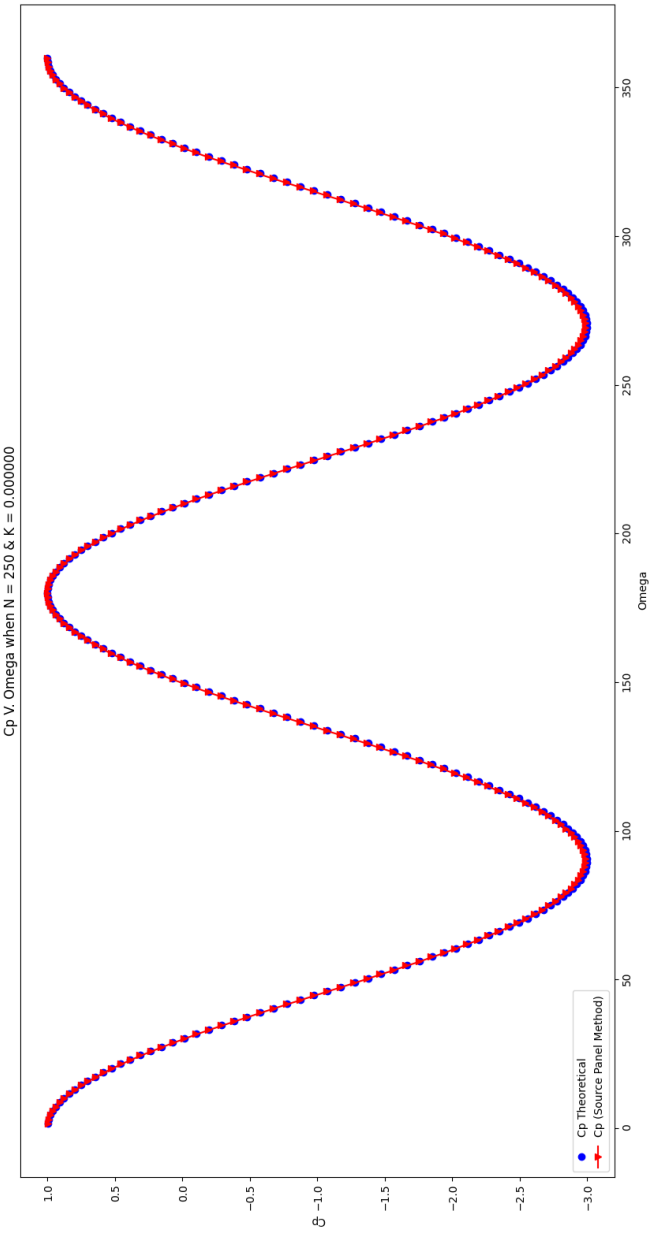

N = 250 and K = -1

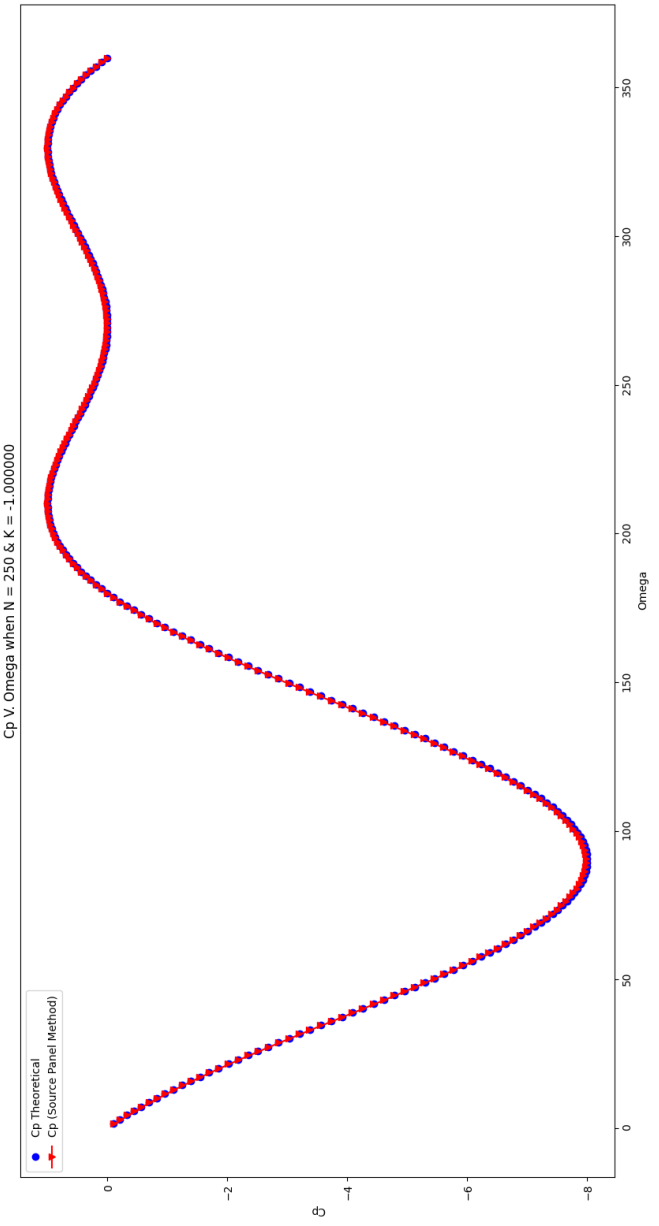
Cp V. Omega when N = 250 & K = -1.000000
Cp Theoretical
Cp (Source Panel Method)
Cp
Omega
0
−2
−4
−6
−8
0
50
100
150
200
250
300
350

N = 250 and K = -2

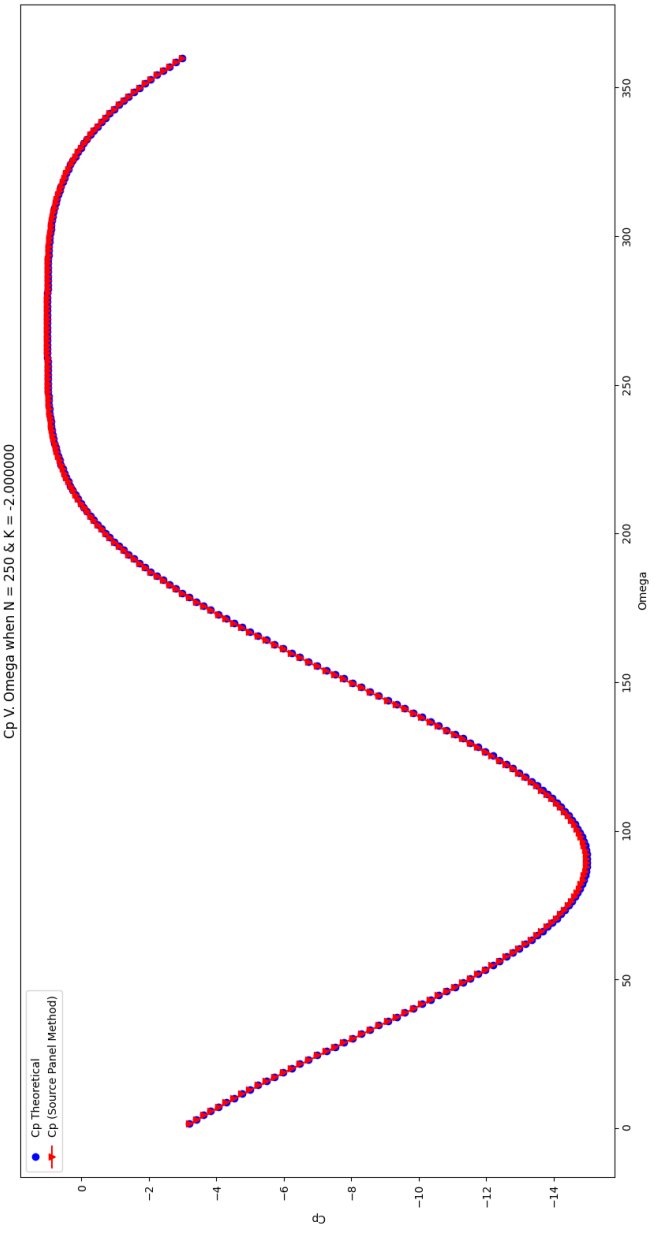
Cp V. Omega when N = 250 & K = -2.000000
Cp Theoretical
Cp (Source Panel Method)
Cp
Omega
0
−2
−4
−6
−8
−10
−12
−14
0
50
100
150
200
250
300
350

N = 250 and K = -3

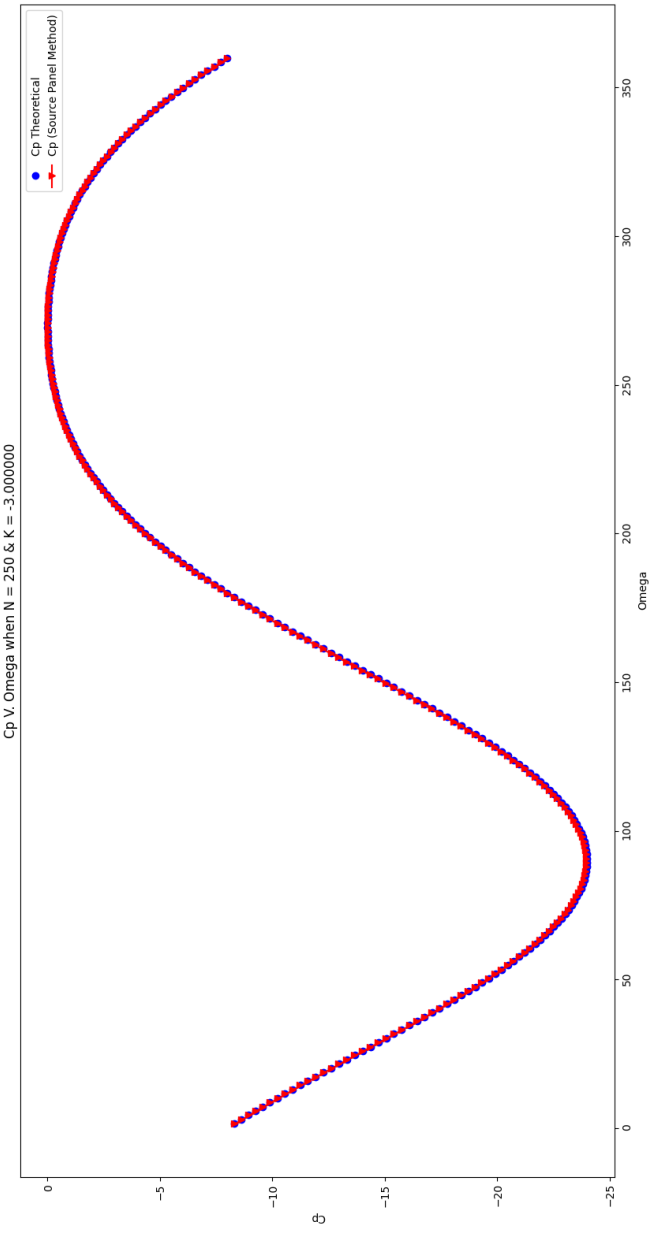
Cp V. Omega when N = 250 & K = -3.000000
Cp Theoretical
Cp (Source Panel Method)
Cp
Omega
0
−5
−10
−15
−20
−25
0
50
100
150
200
250
300
350

3. Table

i	Omega	q	num. Cp	theo. Cp	% error
1	1.44	2.008	-0.103	-0.103	-0.493
2	2.88	2.006	-0.21	-0.211	-0.301
3	4.32	2.002	-0.323	-0.324	-0.376
4	5.76	1.998	-0.44	-0.442	-0.43
5	7.2	1.992	-0.562	-0.564	-0.436
6	8.64	1.986	-0.689	-0.691	-0.382
7	10.08	1.978	-0.821	-0.823	-0.234
8	11.52	1.968	-0.957	-0.958	-0.137
9	12.96	1.958	-1.095	-1.098	-0.287
10	14.4	1.946	-1.241	-1.242	-0.092
11	15.84	1.932	-1.388	-1.39	-0.165
12	17.28	1.918	-1.538	-1.541	-0.207
13	18.72	1.902	-1.692	-1.696	-0.207
14	20.16	1.886	-1.851	-1.854	-0.158
15	21.6	1.867	-2.01	-2.015	-0.214
16	23.04	1.847	-2.172	-2.178	-0.261
17	24.48	1.827	-2.338	-2.344	-0.278
18	25.92	1.805	-2.506	-2.513	-0.26
19	27.36	1.783	-2.678	-2.683	-0.203
20	28.8	1.759	-2.848	-2.855	-0.246
21	30.24	1.735	-3.022	-3.029	-0.24
22	31.68	1.709	-3.194	-3.204	-0.314
23	33.12	1.683	-3.369	-3.38	-0.33
24	34.56	1.655	-3.546	-3.556	-0.276
25	36.0	1.624	-3.725	-3.733	-0.209
26	37.44	1.594	-3.901	-3.91	-0.23
27	38.88	1.562	-4.078	-4.087	-0.22
28	40.32	1.53	-4.25	-4.263	-0.298
29	41.76	1.498	-4.425	-4.438	-0.305
30	43.2	1.464	-4.601	-4.613	-0.255
31	44.64	1.43	-4.773	-4.785	-0.254
32	46.08	1.394	-4.942	-4.957	-0.291
33	47.52	1.355	-5.114	-5.126	-0.227
34	48.96	1.319	-5.277	-5.293	-0.299
35	50.4	1.279	-5.444	-5.457	-0.233
36	51.84	1.241	-5.6	-5.618	-0.324
37	53.28	1.201	-5.762	-5.776	-0.255
38	54.72	1.161	-5.912	-5.931	-0.313
39	56.16	1.118	-6.068	-6.082	-0.236
40	57.6	1.076	-6.211	-6.229	-0.295
41	59.04	1.032	-6.356	-6.372	-0.243
42	60.48	0.99	-6.489	-6.51	-0.311
43	61.92	0.946	-6.623	-6.643	-0.297
44	63.36	0.9	-6.753	-6.771	-0.269
45	64.8	0.855	-6.875	-6.894	-0.279
46	66.24	0.809	-6.99	-7.012	-0.304

47	67.68	0.763	-7.103	-7.123	-0.281
48	69.12	0.715	-7.207	-7.229	-0.31
49	70.56	0.669	-7.307	-7.329	-0.293
50	72.0	0.62	-7.401	-7.422	-0.29
51	73.44	0.572	-7.49	-7.509	-0.251
52	74.88	0.524	-7.566	-7.589	-0.309
53	76.32	0.474	-7.643	-7.663	-0.259
54	77.76	0.426	-7.705	-7.729	-0.32
55	79.2	0.376	-7.763	-7.789	-0.332
56	80.64	0.327	-7.818	-7.841	-0.289
57	82.08	0.277	-7.86	-7.886	-0.331
58	83.52	0.227	-7.903	-7.923	-0.264
59	84.96	0.177	-7.93	-7.954	-0.303
60	86.4	0.127	-7.953	-7.976	-0.293
61	87.84	0.076	-7.967	-7.991	-0.306
62	89.28	0.026	-7.979	-7.999	-0.257
63	90.72	-0.026	-7.979	-7.999	-0.257
64	92.16	-0.076	-7.967	-7.991	-0.306
65	93.6	-0.127	-7.953	-7.976	-0.293
66	95.04	-0.177	-7.93	-7.954	-0.303
67	96.48	-0.227	-7.903	-7.923	-0.264
68	97.92	-0.277	-7.86	-7.886	-0.331
69	99.36	-0.327	-7.818	-7.841	-0.289
70	100.8	-0.376	-7.763	-7.789	-0.332
71	102.24	-0.426	-7.705	-7.729	-0.32
72	103.68	-0.474	-7.643	-7.663	-0.259
73	105.12	-0.524	-7.566	-7.589	-0.309
74	106.56	-0.572	-7.49	-7.509	-0.251
75	108.0	-0.62	-7.401	-7.422	-0.29
76	109.44	-0.669	-7.307	-7.329	-0.293
77	110.88	-0.715	-7.207	-7.229	-0.31
78	112.32	-0.763	-7.103	-7.123	-0.281
79	113.76	-0.809	-6.99	-7.012	-0.304
80	115.2	-0.855	-6.875	-6.894	-0.279
81	116.64	-0.9	-6.753	-6.771	-0.269
82	118.08	-0.946	-6.623	-6.643	-0.297
83	119.52	-0.99	-6.489	-6.51	-0.311
84	120.96	-1.032	-6.356	-6.372	-0.243
85	122.4	-1.076	-6.211	-6.229	-0.295
86	123.84	-1.118	-6.068	-6.082	-0.236
87	125.28	-1.161	-5.912	-5.931	-0.313
88	126.72	-1.201	-5.762	-5.776	-0.255
89	128.16	-1.241	-5.6	-5.618	-0.324
90	129.6	-1.279	-5.444	-5.457	-0.233
91	131.04	-1.319	-5.277	-5.293	-0.299
92	132.48	-1.355	-5.114	-5.126	-0.227
93	133.92	-1.394	-4.942	-4.957	-0.291
94	135.36	-1.43	-4.773	-4.785	-0.254
95	136.8	-1.464	-4.601	-4.613	-0.255
96	138.24	-1.498	-4.425	-4.438	-0.305

97	139.68	-1.53	-4.25	-4.263	-0.298
98	141.12	-1.562	-4.078	-4.087	-0.22
99	142.56	-1.594	-3.901	-3.91	-0.23
100	144.0	-1.624	-3.725	-3.733	-0.209
101	145.44	-1.655	-3.546	-3.556	-0.276
102	146.88	-1.683	-3.369	-3.38	-0.33
103	148.32	-1.709	-3.194	-3.204	-0.314
104	149.76	-1.735	-3.022	-3.029	-0.24
105	151.2	-1.759	-2.848	-2.855	-0.246
106	152.64	-1.783	-2.678	-2.683	-0.203
107	154.08	-1.805	-2.506	-2.513	-0.26
108	155.52	-1.827	-2.338	-2.344	-0.278
109	156.96	-1.847	-2.172	-2.178	-0.261
110	158.4	-1.867	-2.01	-2.015	-0.214
111	159.84	-1.886	-1.851	-1.854	-0.158
112	161.28	-1.902	-1.692	-1.696	-0.207
113	162.72	-1.918	-1.538	-1.541	-0.207
114	164.16	-1.932	-1.388	-1.39	-0.165
115	165.6	-1.946	-1.241	-1.242	-0.092
116	167.04	-1.958	-1.095	-1.098	-0.287
117	168.48	-1.968	-0.957	-0.958	-0.137
118	169.92	-1.978	-0.821	-0.823	-0.234
119	171.36	-1.986	-0.689	-0.691	-0.382
120	172.8	-1.992	-0.562	-0.564	-0.436
121	174.24	-1.998	-0.44	-0.442	-0.43
122	175.68	-2.002	-0.323	-0.324	-0.376
123	177.12	-2.006	-0.21	-0.211	-0.301
124	178.56	-2.008	-0.103	-0.103	-0.493
125	180.0	-2.008	0.0	0.0	-100.0
126	181.44	-2.008	0.098	0.098	-0.469
127	182.88	-2.006	0.19	0.191	-0.272
128	184.32	-2.002	0.278	0.279	-0.323
129	185.76	-1.998	0.36	0.361	-0.351
130	187.2	-1.992	0.437	0.438	-0.336
131	188.64	-1.986	0.509	0.511	-0.278
132	190.08	-1.978	0.577	0.578	-0.161
133	191.52	-1.968	0.639	0.639	-0.088
134	192.96	-1.958	0.695	0.696	-0.173
135	194.4	-1.946	0.747	0.747	-0.052
136	195.84	-1.932	0.793	0.794	-0.085
137	197.28	-1.918	0.834	0.835	-0.097
138	198.72	-1.902	0.871	0.872	-0.088
139	200.16	-1.886	0.903	0.903	-0.06
140	201.6	-1.867	0.93	0.93	-0.071
141	203.04	-1.847	0.952	0.953	-0.073
142	204.48	-1.827	0.97	0.971	-0.063
143	205.92	-1.805	0.984	0.984	-0.045
144	207.36	-1.783	0.993	0.993	-0.023
145	208.8	-1.759	0.999	0.999	-0.013
146	210.24	-1.735	1.0	1.0	0.002

147	211.68	-1.709	0.998	0.997	0.024
148	213.12	-1.683	0.992	0.991	0.049
149	214.56	-1.655	0.983	0.982	0.062
150	216.0	-1.624	0.97	0.969	0.065
151	217.44	-1.594	0.954	0.953	0.092
152	218.88	-1.562	0.936	0.935	0.108
153	220.32	-1.53	0.915	0.913	0.178
154	221.76	-1.498	0.892	0.89	0.216
155	223.2	-1.464	0.866	0.864	0.212
156	224.64	-1.43	0.838	0.836	0.244
157	226.08	-1.394	0.808	0.806	0.322
158	227.52	-1.355	0.777	0.774	0.287
159	228.96	-1.319	0.745	0.741	0.431
160	230.4	-1.279	0.71	0.707	0.382
161	231.84	-1.241	0.676	0.672	0.601
162	233.28	-1.201	0.64	0.636	0.536
163	234.72	-1.161	0.604	0.6	0.743
164	236.16	-1.118	0.566	0.563	0.633
165	237.6	-1.076	0.53	0.526	0.893
166	239.04	-1.032	0.493	0.489	0.833
167	240.48	-0.99	0.457	0.452	1.209
168	241.92	-0.946	0.421	0.415	1.313
169	243.36	-0.9	0.385	0.38	1.356
170	244.8	-0.855	0.35	0.344	1.609
171	246.24	-0.809	0.317	0.31	2.01
172	247.68	-0.763	0.283	0.277	2.147
173	249.12	-0.715	0.252	0.245	2.76
174	250.56	-0.669	0.222	0.215	3.057
175	252.0	-0.62	0.193	0.186	3.586
176	253.44	-0.572	0.165	0.159	3.721
177	254.88	-0.524	0.141	0.134	5.555
178	256.32	-0.474	0.117	0.11	5.767
179	257.76	-0.426	0.097	0.089	8.987
180	259.2	-0.376	0.078	0.07	12.067
181	260.64	-0.327	0.06	0.053	14.096
182	262.08	-0.277	0.046	0.038	22.726
183	263.52	-0.227	0.032	0.025	27.239
184	264.96	-0.177	0.023	0.015	51.872
185	266.4	-0.127	0.016	0.008	98.628
186	267.84	-0.076	0.011	0.003	286.163
187	269.28	-0.026	0.007	0.0	2165.635
188	270.72	0.026	0.007	0.0	2165.635
189	272.16	0.076	0.011	0.003	286.163
190	273.6	0.127	0.016	0.008	98.628
191	275.04	0.177	0.023	0.015	51.872
192	276.48	0.227	0.032	0.025	27.239
193	277.92	0.277	0.046	0.038	22.726
194	279.36	0.327	0.06	0.053	14.096
195	280.8	0.376	0.078	0.07	12.067
196	282.24	0.426	0.097	0.089	8.987

197	283.68	0.474	0.117	0.11	5.767
198	285.12	0.524	0.141	0.134	5.555
199	286.56	0.572	0.165	0.159	3.721
200	288.0	0.62	0.193	0.186	3.586
201	289.44	0.669	0.222	0.215	3.057
202	290.88	0.715	0.252	0.245	2.76
203	292.32	0.763	0.283	0.277	2.147
204	293.76	0.809	0.317	0.31	2.01
205	295.2	0.855	0.35	0.344	1.609
206	296.64	0.9	0.385	0.38	1.356
207	298.08	0.946	0.421	0.415	1.313
208	299.52	0.99	0.457	0.452	1.209
209	300.96	1.032	0.493	0.489	0.833
210	302.4	1.076	0.53	0.526	0.893
211	303.84	1.118	0.566	0.563	0.633
212	305.28	1.161	0.604	0.6	0.743
213	306.72	1.201	0.64	0.636	0.536
214	308.16	1.241	0.676	0.672	0.601
215	309.6	1.279	0.71	0.707	0.382
216	311.04	1.319	0.745	0.741	0.431
217	312.48	1.355	0.777	0.774	0.287
218	313.92	1.394	0.808	0.806	0.322
219	315.36	1.43	0.838	0.836	0.244
220	316.8	1.464	0.866	0.864	0.212
221	318.24	1.498	0.892	0.89	0.216
222	319.68	1.53	0.915	0.913	0.178
223	321.12	1.562	0.936	0.935	0.108
224	322.56	1.594	0.954	0.953	0.092
225	324.0	1.624	0.97	0.969	0.065
226	325.44	1.655	0.983	0.982	0.062
227	326.88	1.683	0.992	0.991	0.049
228	328.32	1.709	0.998	0.997	0.024
229	329.76	1.735	1.0	1.0	0.002
230	331.2	1.759	0.999	0.999	-0.013
231	332.64	1.783	0.993	0.993	-0.023
232	334.08	1.805	0.984	0.984	-0.045
233	335.52	1.827	0.97	0.971	-0.063
234	336.96	1.847	0.952	0.953	-0.073
235	338.4	1.867	0.93	0.93	-0.071
236	339.84	1.886	0.903	0.903	-0.06
237	341.28	1.902	0.871	0.872	-0.088
238	342.72	1.918	0.834	0.835	-0.097
239	344.16	1.932	0.793	0.794	-0.085
240	345.6	1.946	0.747	0.747	-0.052
241	347.04	1.958	0.695	0.696	-0.173
242	348.48	1.968	0.639	0.639	-0.088
243	349.92	1.978	0.577	0.578	-0.161
244	351.36	1.986	0.509	0.511	-0.278
245	352.8	1.992	0.437	0.438	-0.336
246	354.24	1.998	0.36	0.361	-0.351

247	355.68	2.002	0.278	0.279	-0.323
248	357.12	2.006	0.19	0.191	-0.272
249	358.56	2.008	0.098	0.098	-0.469

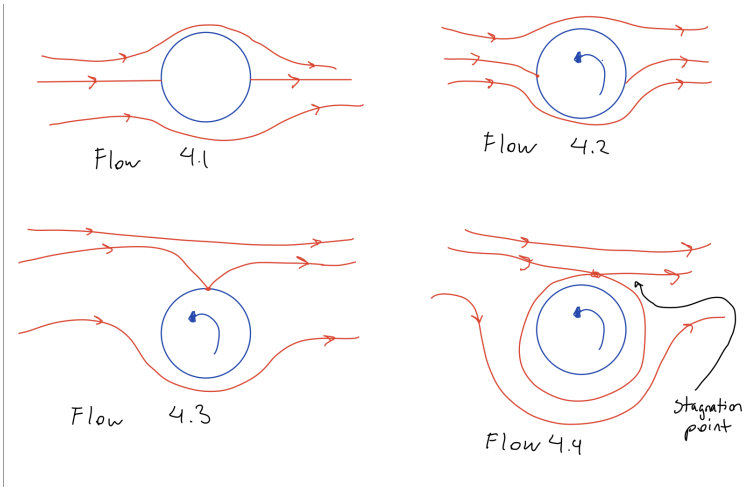

FIGURE 3. Four Flows
Hand Drawn

4. Summary Sketch

As seen from the image above, there are four flows all corresponding to flows studied in class. In clockwise order from the top left,

$$\Gamma = 0 \tag{4.1}$$

$$\frac{\Gamma}{2\pi U a} < 1 \tag{4.2}$$

$$\frac{\Gamma}{2\pi U a} = 1 \tag{4.3}$$

$$\frac{\Gamma}{2\pi U a} > 1 \tag{4.4}$$

From **Flow 4.1** it is clear to see that without circulation values, we have stagnation points at $\theta = 0$ and $\theta = \pi$ when $\Gamma = 0$. As expected, maximum flow speed occurs at the top and bottom of the cylinder where fluid would be anticipated to contour around the surface. According to *Katz and Plotkin*, potential flow theory states that pressure loads at the fore and aft of the cylinder would cancel out. However, in reality there is surface separation towards the rear of the cylinder.

From **Flow 4.2** the effect of circulation begins to make itself apparent. Therefore, depending on the direction of force F_y, one would expect to see a graph as shown. From **Flow 4.3** Circulation of the cylinder begins to show a stagnation point due to the effect of a changing *Cp* as seen in the graphs of the previous section. It does not however, have a proper stagnation point until *Flow 4.4* where circulation causes the stagnation point to appear. Therefore, one may ascertain that circulation of a cylinder will cause significant aerodynamic changes; an idea that will carry on to most other objects. Of course, these graphs seem to add on to results discovered by *Kutta* and *Joukowski*. Though outside the scope of this project, it is also interesting to note that the resultant aerodynamic forces will act normal to the freestream velocity.

5. Streamline Pattern Plots

$\Gamma = 0$ and K = 0

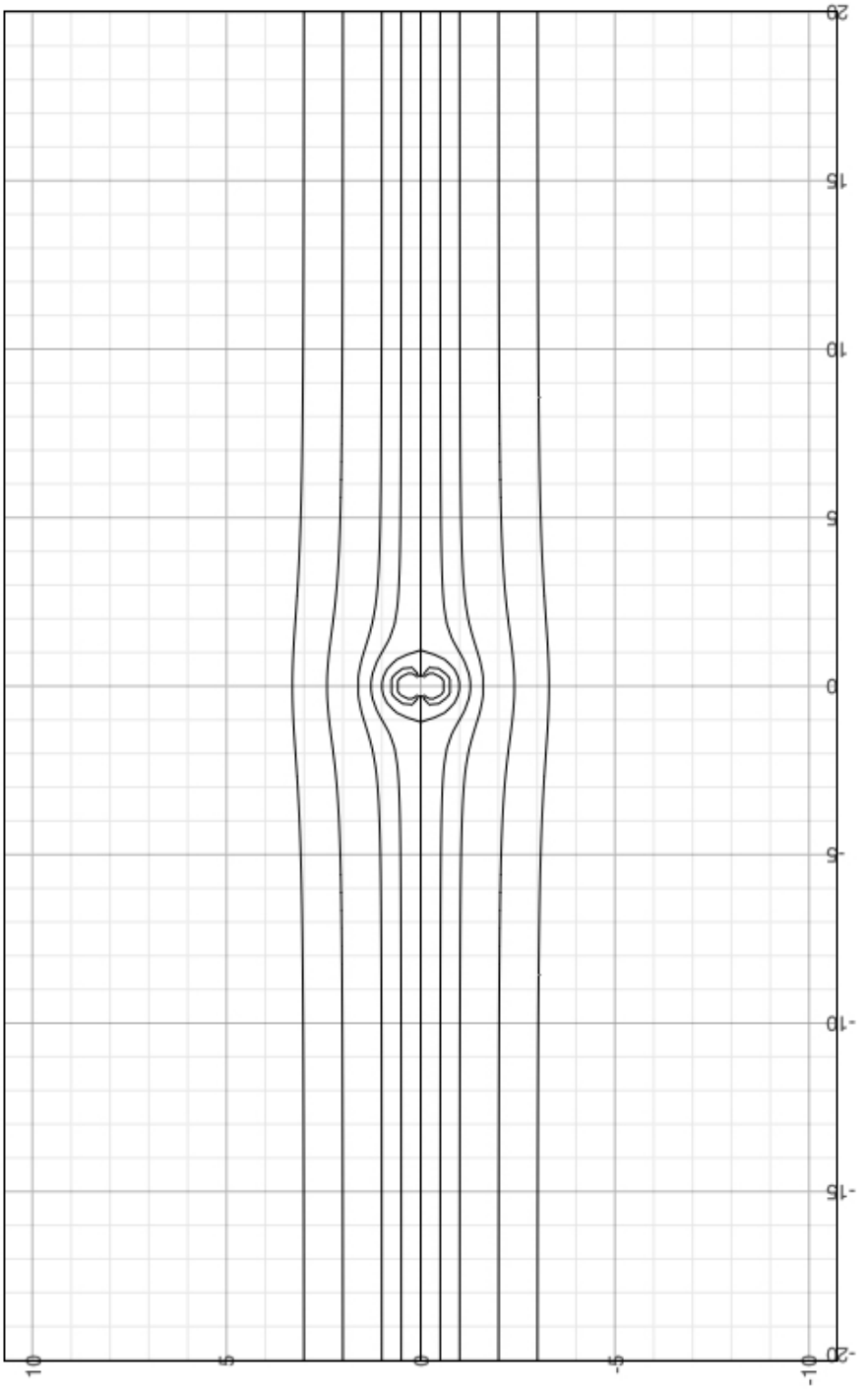

$\Gamma = 2\pi$and K = -1

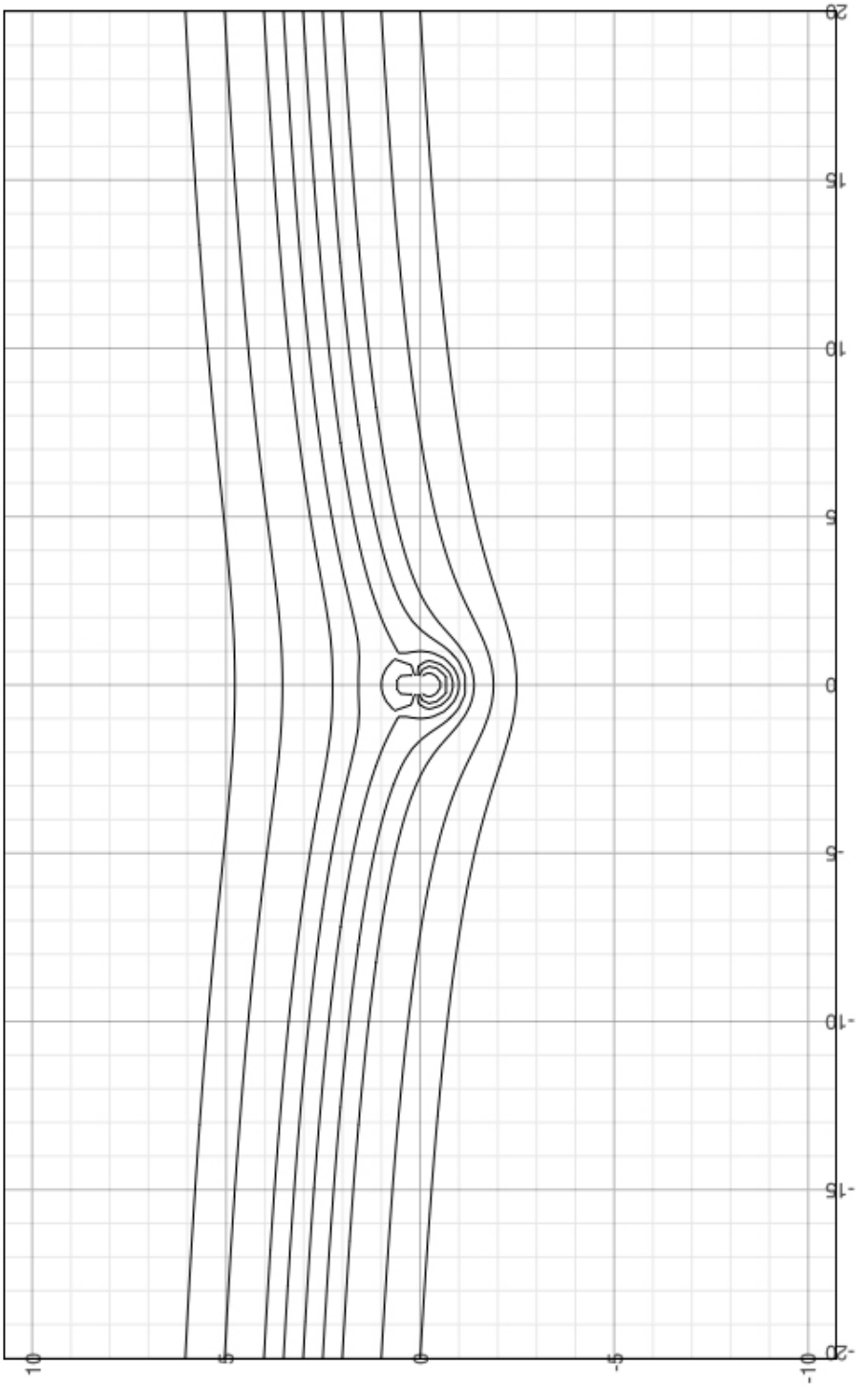

$\Gamma = 4\pi$ and K = -2

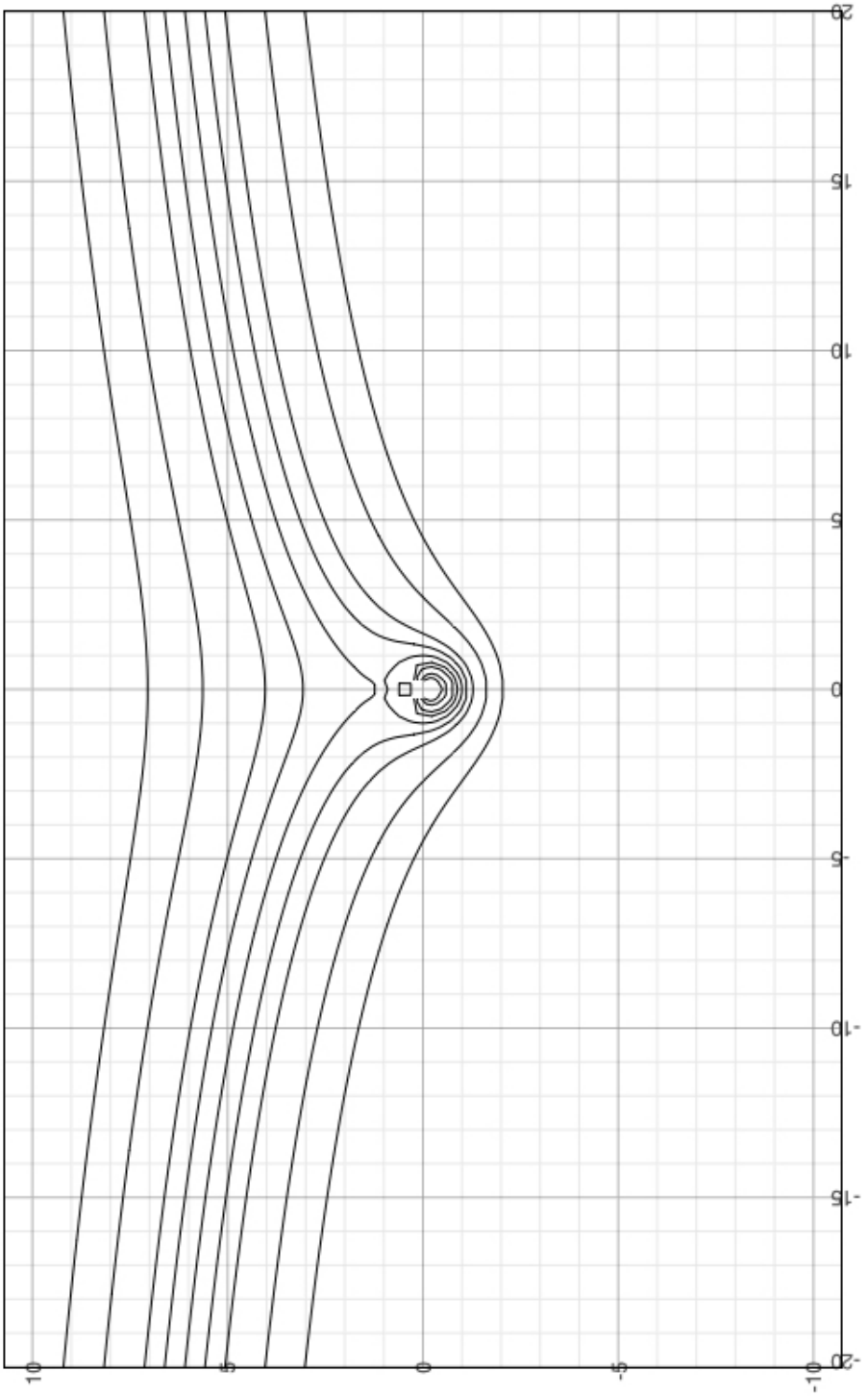

$\Gamma = 6\pi$ and K = -3

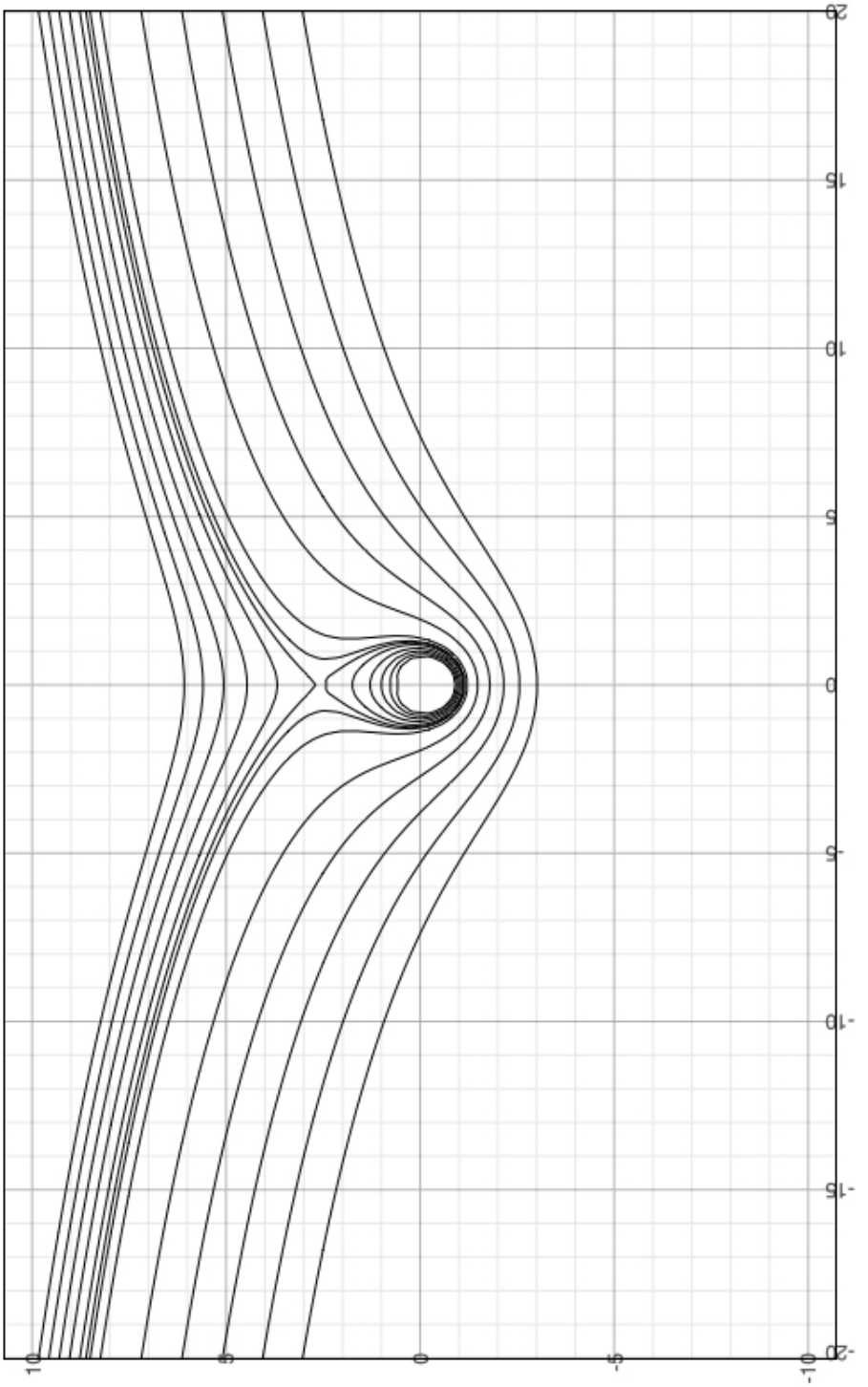

5.1. *Pressure Coefficient Theory V. Actual*
N = 250 and K = 0 With Supercritical and Subcritical Plots

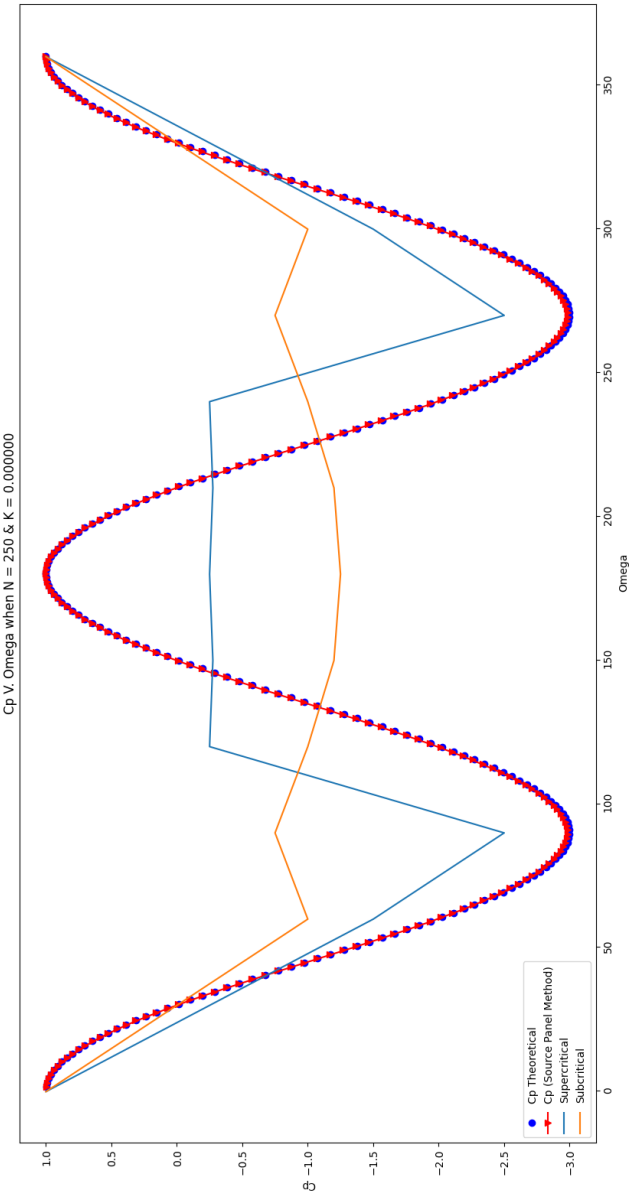

6. Citations

[1] Gerhart, Philip M., et al. Munson, Young, and Okiishi's Fundamentals of Fluid Mechanics. Wiley, 2016. ISBN-13: 978-1119080701

[2] Katz, Joseph, and Allen Plotkin. Low-Speed Aerodynamics. Cambridge University Press, 2010. ISBN 0 521 66219 2

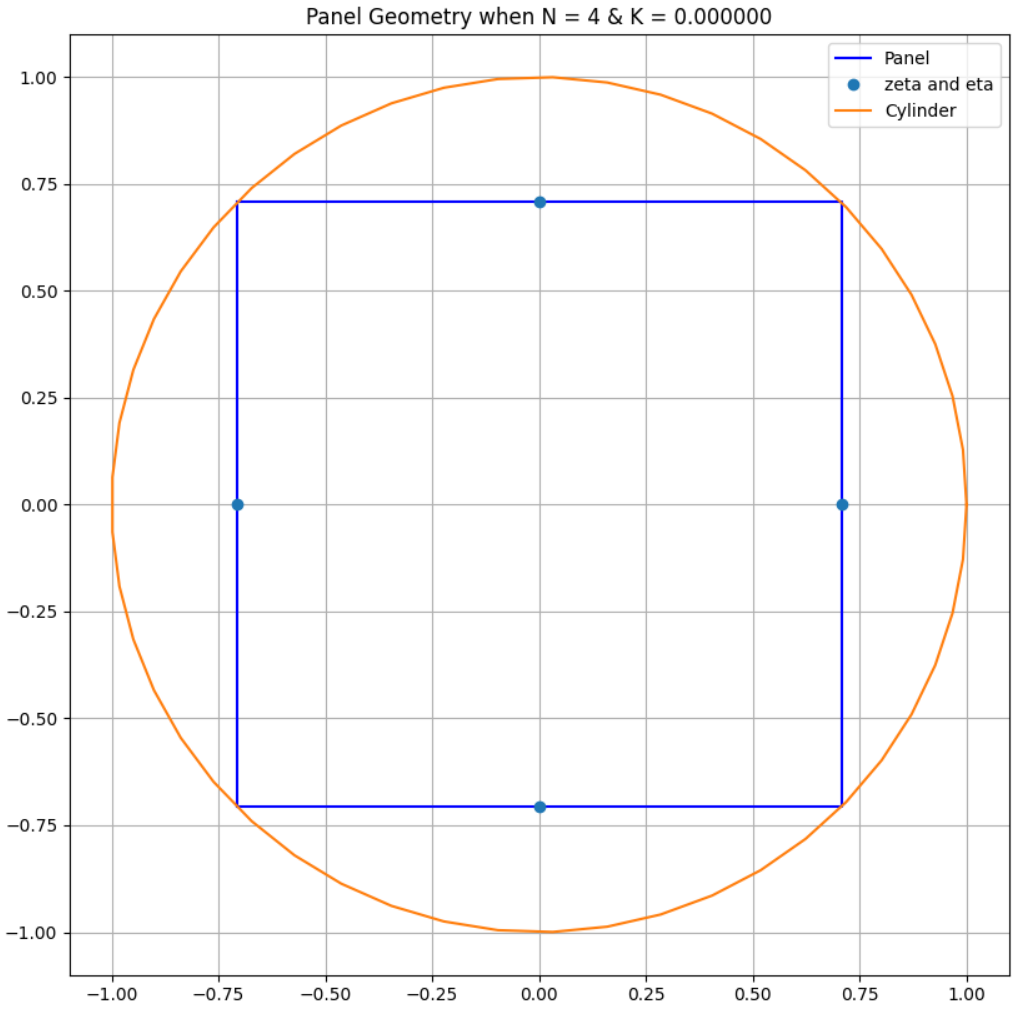

FIGURE 4. Panel Method

Appendix A

Hand Calculations for K = 0 and N = 4
Due to this being a perennial school project, I have omitted the hand work

This Page Left Intentionally Empty

Appendix B

Due to this being a class project attempted by engineering students across the country every year, I will not be including the python code in this text.

For all engineering students attempting this, good luck.